Received on May 2020

Journal of Soft Computing and Engineering Applications

https://srkpublication.org/

An Efficient TSA-RBFNN Technique for Energy Management in Micro Grid Connected System with Renewable Energy Resources

Abisha S. S[1*], Pani Shajini. M[2], Saranya. Y. S[3]

[1]*Department of ECE, Anna University, India*
[2]*Department of ECE, Anna University, India*
[3]*Department of MBA, Anna University, India*
[*]Corresponding author email: Shaa96174@gmail.com

Abstract: In this manuscript, a proficient hybrid approach to the system model and the optimum energy management of the micro-grid with less cost is proposed. The innovative of the proposed method is the consolidation of Tunicate swarm optimization (TSA) and Radial Basis functional Neural Network (RBFNN) known as TSA-RBFNN, which enables the decision making along the multi-objective issues. Furthermore, the most advantages of the TSA-RBFNN technique is the cost-effective power production of the micro-grids (MGs) including effectual use of renewable energy sources (RESs) without lose the obtainable energy. The technique is concerned with more mathematical optimization issues, which involves an objective function that should be optimal concurrently. The TSA algorithm improves the micro-grid structure at minimal fuel cost to carry out the necessary load requirement by utilizing the micro-grids inputs such as wind turbine (WT), photovoltaic (PV) array, micro turbine (MT), energy storage system (ESS) and related cost operation. In TSA-RBFNN technique, RBFNN learning phase is used to forecast the load requirement. In terms of the predicting load requirement, minimal annualized fuel cost properties, cost operation, replacement cost is minimized with every successive point of the TSA-RBFNN technique. The efficiency of the TSA-RBFNN technique is analyzed by likened to the other existing techniques like COA-RNN and BFA-ANN. The comparison outcomes prove the magnificence of the TSA-RBFNN technique; also corroborate its efficient to determine the complex.

Keywords: *Wind turbine, Micro turbine, Operation cost, Photovoltaic, Tunicate swarm optimization, Radial Basis functional Neural Network*

1. INTRODUCTION

The applications of RESs have pointed out in the past years; RES are minimizing the green house gas emissions and fuel usage that are used to contribute in the Distributed Generation (DG) enhancement to highlight the aggressive solution for the future. It means power system connected grid [1, 2]. Thus they can generate electricity with minimal environmental impacts, and easy to install, highly reliable and efficiency increases. In addition, owing to inherent nature of both renewable sources with energy utilized by load, a grid connection is required. Under the circumstances, the energy storage systems (ESS) like flywheels, super

capacitor, batteries etc [3]. And energy management system (EMS) is proposed to enhance system stability and its efficiency. Generally, microgrid (MG) is powerful enough to work in grid-connected as well as stand-alone systems. Those are illustrated as less voltage systems consisting of loads, storage device and distributed generation units, which directly coupled with mains in a single point of common coupling (PCC) [4].

Grid connection in RES can be used to achieve a set of predefined objectives, like reducing grid operating costs or increasing revenues in line with DG auction and electricity market prizes. EMS is responsible for controlling power flows between components [5-7]. In addition, the EMS is based on the grid, the power framework in specific the grid elements energy management potential must be taken into account (control over which sources, loads and storage components). When the power design together with predefined objectives is known, EMS model could carried out using various approaches [8, 9]. For example, in an EMS it is modelled using local forecasting and stochastic dynamic programming (SDP), which is a grid connected MG. Furthermore, the EMS model focuses on controlling the EMS with a predictive control mechanism for compensating the hourly distortions of the energy plan predicted at grid connected micro-grid [10-12].

Battery energy storage (BES) is typically used for solar, wind, turbine power systems; it overcomes the sluggish power requirement. Nevertheless, it is not able to dissipate large power fluctuations when affected by higher frequency [13, 14]. Integrating the application grid with distributed, proficient and dependable DG systems without much investment is still a major challenge. RES have intermissive and approximately fluctuating power, which in turn a primary issue when such source of energy turn a major component of overall grid power generation. This problem can be overcome in principle by massive savings [15]. To overcome the above mentioned issue, the energy saving combination with various phenoms is utilized. The energy storage system is a greater combination of super capacitor (SC) and battery system. Battery energy storage is used to overcome sluggish changing power requirement, whereas SCs handles transient power fluctuations [16, 17]. To prolong the life of the battery and SC, they are not highly charged or discharged. To manage energy reserves at safe operating conditions the EMS is mandatory, in which can efficiently use energy storage and defend against excessive charge or excessive discharge. Here, storage is highly expensive for using large scale; so many researches are work to develop low cost and highly efficient storage devices [18-20]. We develop to research optimal control strategies for energy storage system in grid connection.

In this manuscript, a proficient hybrid approach to the system model and the optimum energy management of the micro-grid along less cost is proposed. The innovative of the TSA-RBFNN method is the consolidation of Tunicate swarm optimization (TSA) and Radial Basis functional Neural Network (RBFNN) known as TSA-RBFNN, which enables the decision making along the multi-objective issues. The remainder of this manuscript is designed as. Segment 2 defines recent research works. Segment 3 portrays problem formulation. Segment 4 delineates the analysis with system configuration of micro-grid connected system for optimum energy management. Segment 5 explains the experimental results. Finally, segment 6 concludes the manuscript.

2. RECENT RESEARCH WORK: A BRIEF REVIEW

Several investigation works have already existed at the literature, which is depending on the energy management in grid connected system with different techniques and aspects. Here, certain works are reviewed.

N. Liu *et al.* [21] introduced a multiple-level energy management system with power requirement was advanced for the Combined heat and power and micro-grid (MG). An optimization modeling of micro-grid operator (MGO) was designed, which includes gas cost, the revenue from the energy sale to the consumer, high electricity to utility grid. The combined heat and power system can be enabled as a hybrid manner, which were followed the electric load (FEL), followed the thermal load (FTL). An optimization model was designed with the use of power consuming, the cost of buying electricity, heat as well as convenient amount of indoor temperature. D. Lifshitz and G. Weiss [22] have suggested three optimal solutions for charging and discharging methods for the increasing the energy at grid connected storage system. The three optimal methods were generated for three versions of the optimization issues. (a) The system contains storage of super capacitor, which has been control in continual time. (b) The system contains battery type storage or super capacitor and has been controlled at a separate time. (c) The system has the storage type of battery and has been controlled in continuous time. D. A. Aviles *et al.* [23] have implemented the concept of less complexity Fuzzy Logic Controller in EMS for grid-connected through MG owing to the RES and storage capability. The main aim of this advanced technique was to reduce the grid power fluctuations due to the battery storage system. The advanced method was employ MG and State of Charge (SOC) both were high/low or maintained power absorbed or delivered. The design parameters were controlled or adjusted to improve the pre-defined characteristics of the MG.

U. Manandhar et al. [24] have developed a novel EMS to the grid connected hybrid energy storage along the super capacitor, battery subject to various operating conditions. The benefits of the new EMS were effectual sharing of power among various ESS, load disturbances, accelerated direct current link voltage controlling for generation and dynamic power sharing amid the grid in terms of battery state of charge (SOC) and battery, minimize the rate of over- charging/discharging of battery current according to

the steady state with fluctuations of transient power, to enhance the power characteristics phenomenon in AC grid as well as seamless mode transitions.

H. Wu *et al.* [25] have implemented the concept of the photovoltaic control strategies, grid-connected inverter with the battery. The new control scheme of EMS to DC bus was implemented to avoid frequent charging or discharging the battery. A linear control function was utilized in external voltage control of the battery to prevent the battery from switching back and forth amid the operating position and the halting position. The example proves the accuracy of the system modeling, control techniques, reaches the transmitting power attached to the stationary grid. This scheme generates a reference to the photovoltaic system participating in power dispatch.

P. Malysz *et al.* [26] have demonstrated the online optimum power control scheme to the function of energy storage in grid-connected through microgrid (MG). The method depending on the mixed-integer-linear program optimization designed for the rolling horizon, while evaluating the future electricity consumers including renewable energy generation. The objective of the performance involves utility-specific objectives related to electricity utilization cost, battery operation costs and peak requirement and load softening. A strong counter-design of the optimization issues has been advanced to manage uncertainty in energy requirement/generation forecasting at compute a proficient way.

J. Pascual et al. [27] have implemented the designing concept of an EMS depend upon less complexity Fuzzy Logic Control (FLC) to grid power profile smooth of grid-connected MG, battery ESS, RESs. The MG power predicts error and the battery state of charge of the new scheme enables the appropriate grid power controlling. The benefits of the new scheme were to reduce the fluctuations, power peaks at the power profile exchange along the grid while retention the energy saved at the battery within safe limitations. The new energy management scheme using generation as well as required predicting to expect the future performance of MG.

2.1. Background of the Research Work

The review of recent investigation work shows that the energy management in the grid connected RESS is an important contribution factor. The EMS design depending upon grid connected, RES including ESS. The energy storage devices like battery, super capacitor, state of charge etc. to enhance the power demand prediction. Integrating the application grid with distributed, proficient and dependable DG systems without much investment is still a major challenge. To overcome the above mentioned issue, the energy saving combination with various phenoms is utilized such as Fuzzy Logic Control (FLC), combined heat and power, SOC etc. FLC is to clarify the grid power profile of grid-connected MG together with battery ESS, RESs. However, it is not able to dissipate with the large power fluctuations when affected by high frequency. To manage energy reserves at secure operating condition, the EMS is mandatory, which can successfully use energy storage and defend against excessive charge or excessive discharge. The advanced EMS uses generation with required predicting to expect the future electricity requirement. At literature, to overcome this problem does not more works are introduced and the revealed works are inefficient. Such problems and constraints have been inspirational to do these research works.

3. PROBLEM FORMULATION

The major purpose of the proposed work as represent at the designing and modeling of grid-connected hybrid energy system. The integration of photovoltaic system, wind turbine, micro turbine, energy storage system denotes the hybrid renewable energy system. To check the cost-effective of the TSA-RBFNN method, the TSA-RBFNN approach finds the optimum number of HRESs. The electricity requirement of the region has been fully meet while minimum energy costs of the system are also reduced under the constraints. The brief explanation of the objective function, operational scheme, execution of the proposed algorithm is given below.

3.1. Formulation of the objective function

The main objective functions in the proposed hybrid renewable energy resources, reduction of annual cost of the overall system. The overall capital cost, replacement cost, cost of operation with maintenance, grid sale, purchase power costs are the factors, which include in the total system cost. These costs involve the installing whereas other costs involve the capital cost [28]. While satisfying other constraints the system with less annual cost is deemed better one. The minimized objective function is as denotes as blow follows,

$$\min(ac) = [n_{PV} c_{PV} + n_{WT} c_{WT} + p_{MT} c_{MT} + p_{ESS} c_{ESS}] \quad (1)$$

where, the total annual cost of photovoltaic, wind turbine, micro turbine, energy storage system are denoted as CPV; CWT; CMT and CESS and AC is denoted as the system annual cost. Annually, overall price of electricity sold for grid ($/yr). The several components which are annual capital cost, annual operational, annual replacement cost comprises each component in the annualized cost. To posses all kind of costs the micro turbine cost analysis is also delineated. The below expression denotes the AC of MT CMT includes few components as follows,

$$c_{MT} = c_{ac(cap)}^{MT} + c_{ac(rep)}^{MT} + c_{f}^{MT} \quad (2)$$

where CMT (f) implies operational (fuel) cost, the annual

replacement cost is denoted as CMT, CMT (f) refers operational (fuel) cost and the annual capital cost is represented as CMT.

3.2. Annualized capital cost

The capital cost of the components involves the components of install and purchase cost. This chapter is mentioned about every component like photovoltaic, wind turbine, micro turbine, energy storage system the annualized capital cost of these components are computed using CRF [29]. To compute the current value of money is the CRF ratio. The overall micro turbine system is revealed as below,

$$c_{ac(cap)}^{MT} = c_{cap)}^{MT} CRF(\alpha, \beta) \tag{3}$$

where, the lifetime indicates β years, rate of interest indicates α then the wind turbine initial capital cost is exhibited as CMT Cap. Therefore the CRF is evaluated as follows below,

$$CRF(\alpha, \beta) = \frac{\alpha(1+a)^{\beta}}{(1+\alpha)^{\beta-1}} \tag{4}$$

3.3. Annual replacement cost

The annual replacement cost of wind turbine implicates replacement cost of wind turbines lifespan. The expression of CMT the annual value of overall replacement cost is described as below,

$$c_{ac(rep)}^{MT} = CRF(\alpha, \beta) = \frac{\alpha(1+a)^{\beta}}{(1+\alpha)^{\beta-1}} \tag{5}$$

where, I specify lifespan of micro turbine system at years and the component replacement cost represents CMT rep. The expression of the remaining power is given below,

3.4. Operational strategy

Due to the environmental issues, the power generated from the photovoltaic panels as well as wind turbine is placed in first priority than micro turbine in the operational strategy. The power management is carried out through the given operational strategy at the proposed grid-connected hybrid system [30]. At the initial stage of this strategy, when the power generated by photovoltaic, wind turbine are sufficient and higher than load requirement, the remainder power could be transferred to the grid, which could be supplied directly by the solar and wind power, it is demonstrated in the equation below,

$$p_{gs}(T) = (p_{PV}(T) + p_{WT}(T) - p_L(T)) \tag{6}$$

here, P defines power supplied to the grid. The operational strategy at the second stage, when the Pgs greater than Pmax gp (maximum grid sales ability) the excessive power is discharged and it is expressed below,

$$p_d(T) = (p_{PV}(T) + p_{WT}(T) - p_L(T) - p_{gp}^{Max} \tag{7}$$

where, Pgp signifies amount of power supplied to the grid. At the third level of the operational strategy, the power from photovoltaic panels is not sufficient when the load could be supplied directly through the grid power that is exhibited in the equation below,

$$p_L(T) \le p_{gp}^{Max} \tag{8}$$

The operational strategy at the fourth stage wind turbine power while the power from the photovoltaic panels and the wind turbine are insufficient when the micro turbine is start and load supplied by micro turbine, grid and photovoltaic. The operational strategy at the fifth stage within a maximal limitation of grid sale ability, the remaining power sold to the grid.

4. ANALYSIS AND SYSTEM CONFIGURATION OF MICRO-GRID CONNECTED SYSTEM FOR OPTIMUM ENERGY MANAGEMENT

In this manuscript, with MG connected systems a proficient control method is proposed for optimal energy management. The proposed technique is TSA-RBFNN technique where the proficient control strategy is the consolidation of TSA and RBFNN [31]. The systems of photovoltaic, wind turbine, micro turbine, energy storage system are the compilation of micro-grid connected system. The power flow control amid the source of energy and the grid is the primary objective of TSA-RBFNN method. This can be satisfying the required power grid from the renewable energy power with grid operator. The power required for the grid operator is provided as a reference to the MG input [32]. The full power reference amid the system parts is accurately distributed through the TSA-RBFNN method. To continuous perform in steady as well as stable output power, the renewable power system units are firmed and allowed by the battery, which performs as the source of energy. Figure 1 portrays the system configuration of the micro-grid connected system.

Figure 1 portrays the dispatchable resources termed as micro turbine, the non-dispatchable resources like photovoltaic, wind turbine, RESs. As seen from this Figure, the battery defines energy storage device. To micro-grid system, the TSA-RBFNN method is utilized to define the EMS and also access the total production of cost operations [33]. The micro-grid energy management is analyzed at the grid-connected method to the distinct function. At the

initial, the control tasks are executed after that micro-grid has been able to plan with the proper ratings. During the micro-grid process the load requirement satisfied all time subject to grid mode. Optimization algorithms are used to express the objective of micro-grids to achieve the optimal function. The power produced from the non-dispatchable resources like photovoltaic, wind turbine is used the energy storage with natural benefit. The dynamic power, operation condition of energy storage system, dispatchable units is deemed as the control aspects utilized to define the energy management scheme [34]. In the TSA-RBFNN technique, the objective function is analyzed in terms of annual capital cost, annual replacement cost, operational cost of the micro-grid system. Here, the procedure with optimum intensity of control units are estimated in provided time. The optimum cost of power controlling is the primary objective of the TSA-RBFNN technique. So, the aim of the micro-grids is to minimize and maximize revenues when the optimal function is attained. The TSA and RBFNN methods are described below.

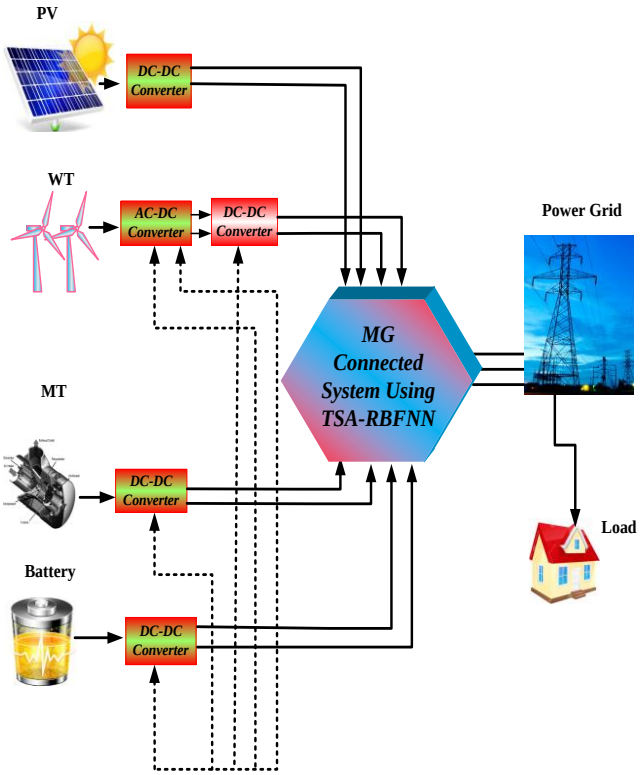

Figure 1: System configuration of MG with proposed TSA-RBFNN Technique

4.1. Aim of Adopting the Proposed TSA Technique

TSA is a meta-heuristic optimization algorithm it follows jet propulsion with swarm behavior of tunicates when the process of navigation and foraging. Tunicate contains capacity to identify the location of food source at the sea [35]. Nevertheless, nothing is known about the food source in a given search location. In this manuscript, to detect the food source two tunicate behaviors are applied, that is optimal. Such behaviors are known as jet propulsion together with swarm intelligence. To mathematical model of jet propulsion behavior, a tunicate must satisfy three different terms. They are, neglect the conflicts among the search agents, movement towards the position of best search agent, remain near to the best search agent. The swarm behavior would update the other search agent positions about the optimum solution. In this manuscript, TSA algorithm is applied to obtain the optimal mean error value so that using this, the speed and torque of the motor can be controlled. Initially, error signals are initialized and randomly generated the gain parameters of the proportional integral controller.

4.1.1. Step by Step TSA process

Step 1: Initialization of population

Initialize the tunicate population $\overrightarrow{P_p}$ which is generated randomly in the search space.

Step 2: Select the initial parameters with maximal count of iterations.

Step 3: Fitness Evaluation

Compute every search agent fitness value. To get minimal error function, the given equation is utilized to achieve the optimal pulses,

$$Fitness = \min(E) \tag{10}$$

Based on the fitness value, the minimum error value is denoted as (E).

Step 4: After calculating the value of fitness, better search agent is examined at the following search space

Step 5: Updating the position of each search agent utilizing the equation (1)

$$\overrightarrow{P_p(x+1)} = \frac{P_p\overrightarrow{(x)} + P_p\overrightarrow{(x+1)}}{2+C_1} \tag{11}$$

Step 6: New Position Updation

Consider the given equation to generate the new solution utilizing crossover as well as mutation operator,

$$NP = R + V \tag{12}$$

here, reflection as *R*, visibility as *V*. Crossover and mutation operator improves the new solution update to obtain an

optimum global solution.

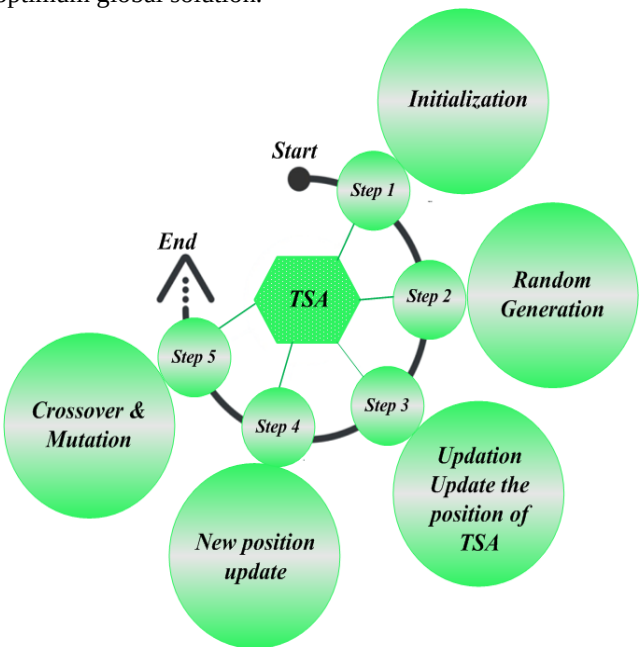

Figure 2: Flow chart of TSA

Step 7: Modify the updating search agent beyond the boundaries of provided search location.

Step 8: Calculate updating the fitness value of search agent if it is best solution than the existing optimum solution.

Step 9: If the stopping criteria is fulfilled, then stop the algorithm. Else, repeat steps 5–8.

Step 10: Return better optimum solution that is acquired so far.

4.2. Prediction of Load Demand Using RBFNN

RBFNN is an artificial neural network that uses radial basis functions as activation functions in the field of mathematical modeling. Input layer is the first layer, and it is consisted of source node to the input data [36]. Single hidden layer in network is the second layer that is carried out the radial basis operations. The nonlinear transformation is used by such functions from the input layer to the hidden layer. The output layer is the third layer. The network's output layer is a linear combination of inputs and neuron parameters radial basis functions. Here, RBFNN is trained with the suitable input time intervals of the day due to target power requirement. To implement the proposed technique, input variables selection for every node refers to first layer then the output is calculated using Gaussian membership function.

Step 1: **The Input Vector**

At the input layer of the network, the input vector a is used. In the TSA-RBFNN technique, the time interval T represents network input, load requirement represents network output. The equation for the input vector is given by,

$$a = \left[a_1 \;\; a_2 \cdots a_p \;\right]^T \tag{13}$$

where, a implies the input vector of the RBFNN.

Step 2: **The RBF Neurons**

Every RBF neuron saves a "prototype" vector. Every RBF neuron compares the input vector with its prototype; also output the value amid 0 and 1, which is a similarity measure. If the input is equal to the prototype the RBF neuron output indicates 1. The value of the neuron's response is known as "activation" value. The prototype vector is known as neuron's "center'.

Step 3: **The Output Nodes**

The network output contains set of nodes; every output node calculates a score sort to the corresponding group. Generally, a classification is carried out by allocating input to the highest scoring group. From each RBF neuron consider the weighted sum of the activation values, the score is computed. In each RBF neuron an output node connects the weighted value by weighted sum and multiplies the activation of the neuron by this weight before adding to the total response. Every output node contains their own set of weights to various categories since every output node calculates the score. The output node provides positive weight to the RBF neurons, whereas negative weight is shared by others.

Step 4: **RBF Neuron Activation Function**

Every RBF neuron calculates a similarity measure between the input and its prototype vector. Input vector is congruent for prototype that gives outcomes nearer to 1. There are various feasible selections of congruent functions depending upon Gaussian. The Gaussian equation of one-dimensional input is signified given below.

$$f(a) = \frac{1}{\alpha\sqrt{2\pi}} e^{-\frac{(a-\beta)^2}{2\alpha^2}} \tag{14}$$

here, input denotes a, mean indicates β, standard deviation refers α. The function of RBF neuron activation is marginally different, it is expressed as:

$$\psi(a) = e^{-\eta\|a-\beta\|^2} \tag{15}$$

here, β implies distribution mean at the Gaussian

distribution.

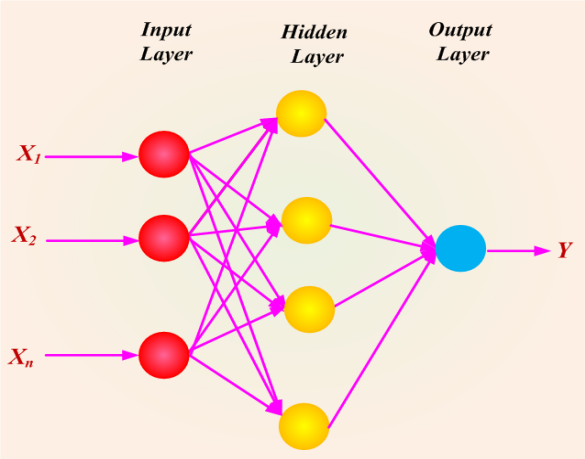

Figure 3: Flow chart of RBFNN

After finishing the algorithm, RBFNN is efficient to forecast controller gain parameters as well as generates combination of optimal solution based on input time interval.

5. RESULT AND DISCUSSION

The TSA-RBFNN approach is performed in MATLAB/Simulink platform. Photovoltaic, wind turbine, battery sources are utilized to meet the load required of the system. The increasing requirement is satisfied using the optimum micro-grid configuration derived from TSA-RBFNN approach. RBFNN approach is explored to assess the combination of optimum micro-grid configuration to satisfy the load requirement; whilst TSA reduces the costs for micro-grid combination like annualized capital cost, operation and replacement cost. The PV power with 24 hour plot is depicted in Figure 4 (a). During the 24-hour periods, the maximum power demand attains 25KW at 14 hrs a day and step by step decreases the power. The cost analysis in PV per day is represented in Figure 4 (b). Here, during the initial period cost analyzed o.19$ at the time period of 0-8hrs; at the time instant of 8-18 hrs the maximum cost attains 0.2$.

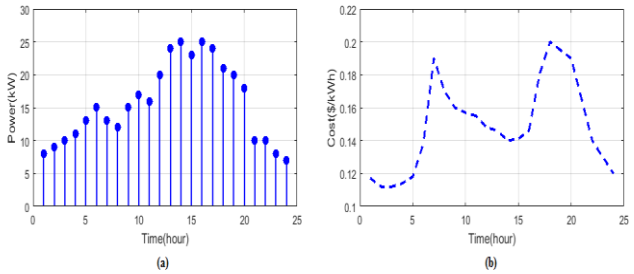

Figure 4: Load requirement of the proposed method for one day (a) Load requirement (b) Cost Profile

Case 1: 1 PV 2WT, ESS and Grid

In case 1, the PV analysis of power generated is represented in Figure 5. Sub plot 5(a) denotes PV power PV_1 and PV_2 are analyzed in a day. When compared to the PV_1 and PV_2, PV_1 is better performing to PV_2. Sub plot 5 (b) denotes wind power WT_1 and WT_2 are analyzed in a day. When compared to the WT_1 and WT_2, WT_1 is better performing to WT_2. Sub plot 5(c) shows the battery charging and discharging period per day. Sub plot 5 (d) delineates the grid power; it attains maximum power of 2.5 KW at 21 hrs per day. Figure 6 implicates the training with testing process of TSA-RBFNN technique per day. Sub plot 6(a) implies the PV_1 power testing and training, the maximum testing occurs 6 KW during the period of 12 hrs; the maximum testing attains 6.2 KW at 12 hrs per day. Sub plot 6(b) depicts the PV_2 power testing and training, the maximum testing occurs 6.2 KW during the period of 13 hrs; the maximum testing attains 6.2 KW at 13 hrs per day. Sub plot 6(c) represents the WT_1 power testing and training, the maximum testing occurs 7.8 KW during the period of 18 hrs. The maximum testing attains 8 KW at 18 hrs per day. Sub plot 6(d) reveals the WT_2 power testing and training, the maximum testing occur 7.6 KW during the period of 12 hrs; the maximum testing attains 7.8KW at 12 hrs per day.

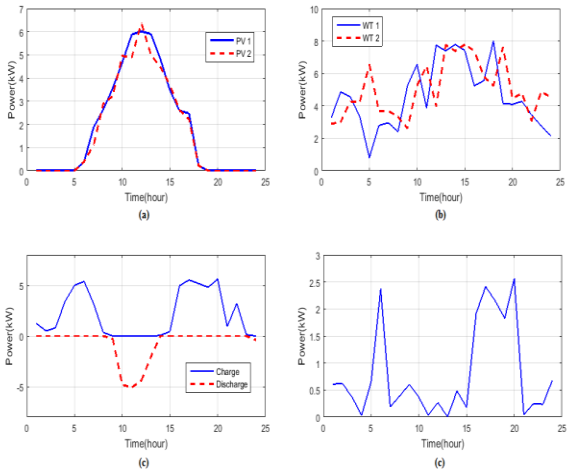

Figure 5: PV Analysis of power generated (a) PV (b) WT (c) ESS (d) Grid Power

Figure 7 displays the individual power in PV_1, PV_2, WT_1, and WT2, battery and grid system. Sub plot 7 (a) refers the individual power in ECO-ANN technique. The maximum PV_1 power attains 6 KW at 0-14 hrs in a day. PV_2 attains the maximum power of 5.8 KW at 0-14 hrs in a day. The maximum WT_1 power attains 7 KW at 0-14 hrs in a day. WT_2 attains the maximum power of 6.8 KW at 0-14 hrs in a day. The battery charging time is 0-8 hr, charged power range is 5 KW at 6hrs. The battery discharge time is 8-15 hrs; it reached maximum discharged power is -5 KW at the time period of 10 hrs. The maximum grid power attains 2.5

KW at 20 hrs. Sub plot 7(b) shows the individual power of CHO-RNN technique. The maximum PV_1 power attains 6 KW at 0-14 hrs in a day. PV_2 attains the maximum power of 5.8 KW at 0-14 hrs in a day. The maximum WT_1 power attains 7 KW at 0-14 hrs in a day. WT_2 attains the maximum power of 6.8 KW at 0-14 hrs in a day. The battery charging time is 0-8 hr, charged power range is 5 KW in 6hrs. The battery discharge time is 8-15 hr; its reached maximum discharge power is -5 KW at the time period of 10 hr. The maximum grid power attains 2.5 KW at 20 hrs. Sub plot 7 (c) displays the individual power of TSA-RBFNN technique. The maximum PV_1 power attains 6 KW at 0-14 hrs in a day. PV_2 attains the maximum power of 5.8 KW at 0-14 hrs in a day. The maximum WT_1 power attains 7 KW at 0-14 hrs in a day. WT_2 attains the maximum power of 6.8 KW at 0-14 hrs in a day. The battery charging time is 0-8 hr, charged power range is 5 KW at 6hrs. The battery discharge time is 8-15 hr; it reached maximum discharged power is -5 KW at the time period of 10 hrs. The maximum grid power attains 2.5 KW at 20 hrs.

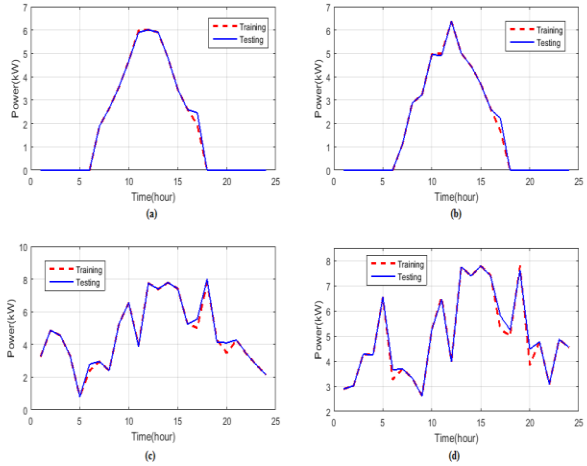

Figure 6: Training & Testing of RBFNN (a) PV1 (b) PV2 (c) WT1 (d) WT2 Power

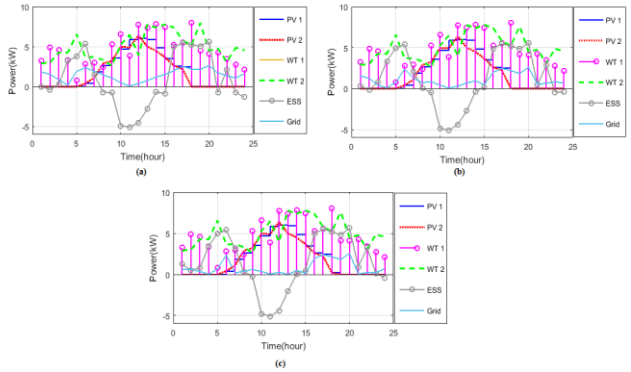

Figure 7: Individual Power (a) EHO-ANN, (b) CHO-RNN, (c) TSA-RBFNN

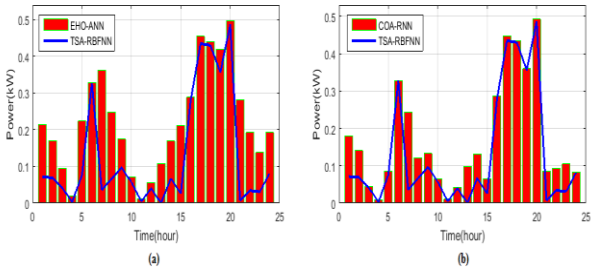

Figure 8: Cost Comparison (a) TSA-RBFNN with EHO-ANN (b) TSA-RBFNN with CHO-RNN

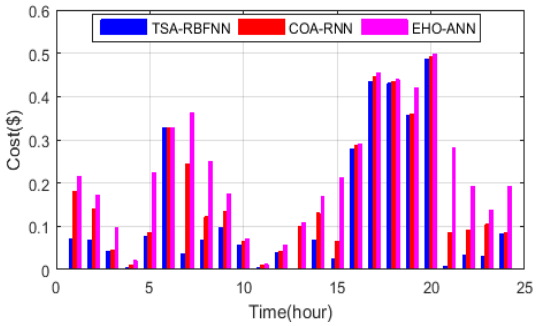

Figure 9: Cost Comparison of proposed and existing technique

Figure 8 illustrates the cost comparison of different techniques. Sub plot 8 (a) signifies the cost comparison analysis of TSA-RBFNN with EHO-ANN, compare to this in our proposed TSA-RBFNN gives the better result. Sub plot 8 (b) depicts the cost comparison analysis of TSA-RBFNN with CHO-RNN; compare to this in our proposed TSA-RBFNN gives the better result. Figure 9 represents the cost comparison of TSA-RBFNN with existing approaches. Here, the cost comparison of TSA-RBFNN and the existing techniques like COA-RNN and EHO-ANN are presented. When likened with existing techniques the cost of TSA-RBFNN technique is low.

Case 2: Absence of PV

In case 2, PV analysis of power generated is represented in Figure 10. Sub plot 10 (a) represents PV power PV_1 and PV_2 are analyzed in a day. When compared to the PV_1 and PV_2, PV_1 is better performing to PV_2. Sub plot 10 (b) indicates wind power WT_1 and WT_2 are analyzed in a day. When compared to the WT_1 and WT_2, WT_1 is better performing to WT_2. Sub plot 10 (c) shows the battery charging and discharging period of per day. Sub plot 10 (d) illustrates the grid power; it attains maximum power of 2.5 KW at 21 hrs per day. Figure 11 implies the training with testing process of TSA-RBFNN technique in a day. Sub plot 11 (a) refers the PV_1 power testing and training, the maximum testing occur 6 KW during the period of 12 hrs, the maximum testing attains 6.2 KW at 12 hrs per day. Sub plot 11 (b) indicates the PV_2 power testing and training, the

maximum testing occur 6.2 KW during the period of 13 hrs, the maximum testing attains 6.2 KW at 13 hrs per day. Sub plot 11 (c) implicates the WT_1 power testing and training, the maximum testing occurs 7.8 KW during the period of 18 hrs. The maximum testing attains 8 KW at 18 hrs per day.

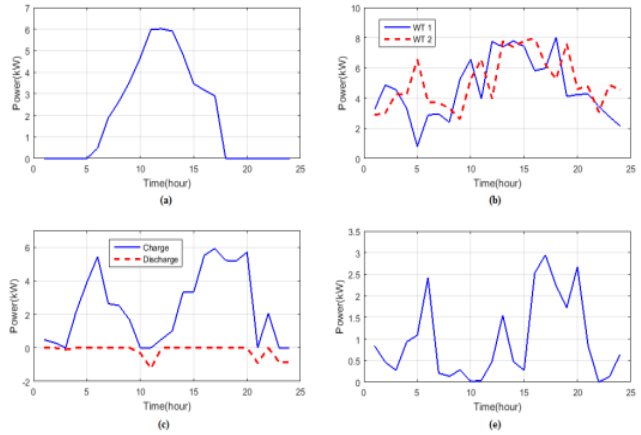

Figure 10: power of (a) PV (b) WT (c) ESS (d) Grid

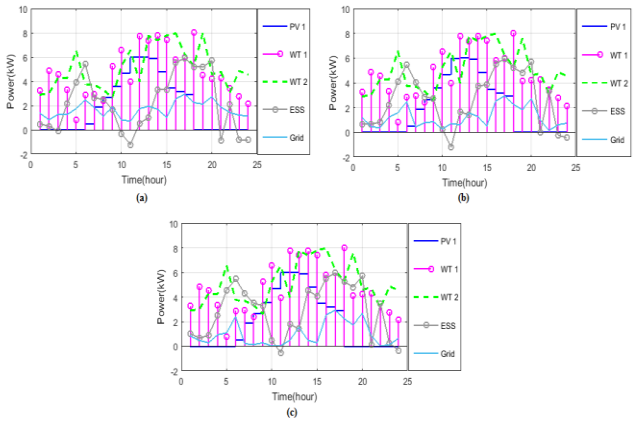

Figure 11: Individual Power (a) EHO-ANN (b) CHO-RNN (c) TSA-RBFNN

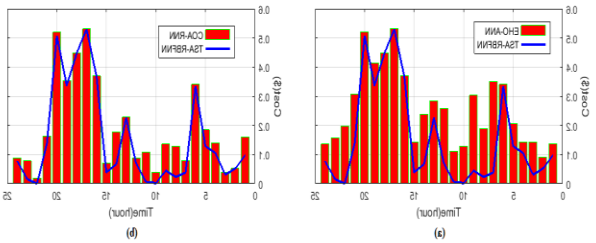

Figure 12: Cost Comparison (a) TSA-RBFNN with EHO-ANN (b) TSA-RBFNN with CHO-RNN

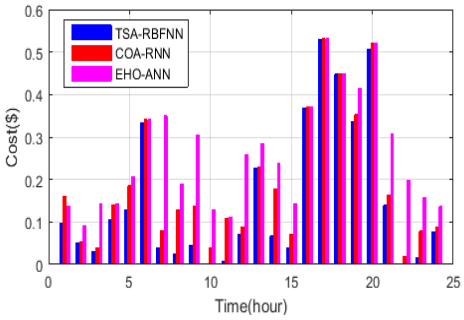

Figure 13: Cost Comparison of proposed with existing technique

Figure 12 illustrates the cost comparison of different techniques, sub plot 12 (a) shows the cost comparison analysis of TSA-RBFNN with EHO-ANN, and compare to this in our proposed TSA-RBFNN gives the better result. Sub plot 12 (b) signifies the cost comparison analysis of TSA-RBFNN with CHO-RNN, compare to this in our proposed TSA-RBFNN gives the better result. Figure 13 displays the cost comparison of TSA-RBFNN with existing approaches. Here, the cost comparison of TSA-RBFNN and the existing techniques like COA-RNN and EHO-ANN are presented. When likened with existing techniques the cost of proposed TSA-RBFNN technique is low.

Case 3: Absence of wind

In case 2, PV analysis of power generated is represented in Figure 14. Sub plot 14 (a) depicts PV power of PV_1 and PV_2 are analyzed in a day. When compared to the PV_1 and PV_2, PV_1 is better performing to PV_2. Sub plot 14(b) implies wind power of WT_1 and WT_2 are analyzed in a day. When compared to the WT_1 and WT_2, WT_1 is better performing to WT_2. Sub plot 14(c) shows the battery charging and discharging period in a day. Sub plot 14 (d) illustrates the grid power; it attains the maximum power of 2.5 KW at 21 hrs in a day. Figure 15 delineates the training with testing process of TSA-RBFNN technique in a day. Sub plot 15 (a) depicts the PV_1 power testing and training, the maximum testing occur 6 KW during the period of 12 hrs. The maximum testing attains 6.2 KW at 12 hr per day. Sub plot 15 (b) depicts the PV_2 power testing and training, the maximum testing occur 6.2 KW during the period of 13 hrs. The maximum testing attains 6.2 KW at 13 hrs per day. Sub plot 15 (c) defines the WT_1 power testing and training, the maximum testing occurs 7.8 KW during the period of 18 hrs. The maximum testing attains 8 KW at 18 hrs per day. Sub plot 15 (d) implicates the WT_2 power testing and training, the maximum testing occur 7.6 KW during the period of 12 hrs. The maximum testing attains 7.8KW at 12 hrs per day.

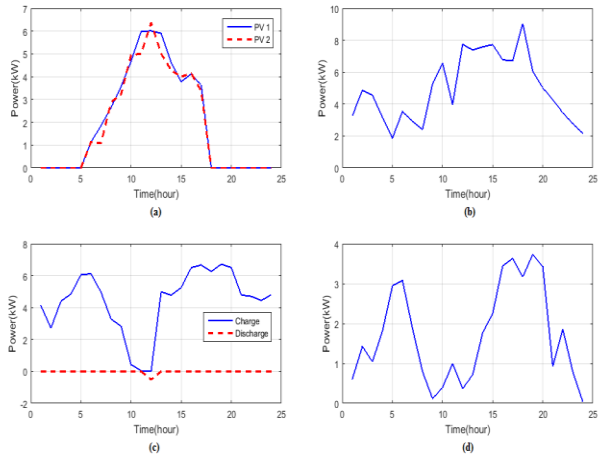

Figure 14: Power analysis of (a) PV Power (b) WT Power (c) ESS Power (d) Grid Power

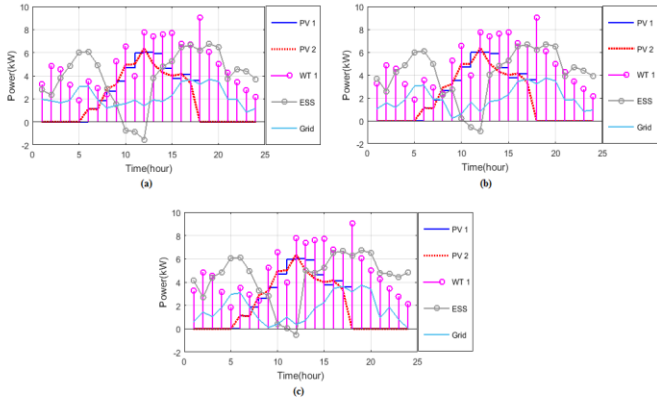

Figure 15: Individual Power of (a) EHO-ANN (b) CHO-RNN (c) TSA-RBFNN

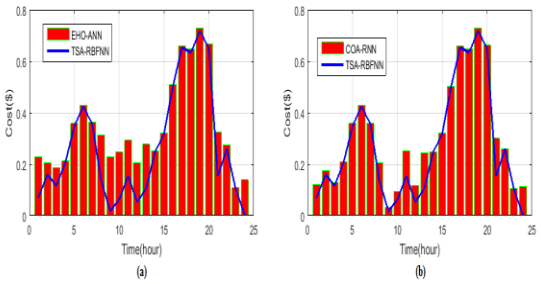

Figure 16: Cost Comparison of (a) TSA-RBFNN with EHO-ANN (b) TSA-RBFNN with CHO-RNN

Figure 16 depicts the individual power of PV_1, PV_2, WT_1, and WT2, battery and grid system. Sub plot 16 (a) shows the individual power of ECO-ANN technique. The maximum PV_1 power attains in 6 KW at 0-14 hrs in a day. PV_2 attains the maximum power of 5.8 KW at 0-14 hrs per day. The maximum WT_1 power attains in 7 KW at 0-14 hrs in a day. WT_2 attains the maximum power of 6.8 KW at 0-14 hrs in a day. The battery charging time is 0-8 hrs, charged power range is 5 KW at 6hrs. The battery discharge time is 8-15 hrs; it reached maximum discharged power is -5 KW at the time period of 10 hrs. The maximum grid power attains in 2.5 KW at 20 hrs. Sub plot 16 (b) represents the individual power of CHO-RNN technique. The maximum PV_1 power attains in 6 KW at 0-14 hrs in a day. PV_2 attains the maximum power of 5.8 KW at 0-14 hrs in a day. The maximum WT_1 power attains in 7 KW at 0-14 hrs in a day. WT_2 attains the maximum power of 6.8 KW at 0-14 hrs in a day. The battery charging time is 0-8 hr, charged power range is 5 KW at 6hrs. The battery discharge time is 8-15 hr; it reached maximum discharged power is -5 KW at the time period of 10 hrs. The maximum grid power attains 2.5 KW at 20 hrs. Sub plot 16 (c) portrays the individual power of TSA-RBFNN technique. The maximum PV_1 power attains 6 KW at 0-14 hrs in a day. PV_2 attains the maximum power of 5.8 KW at 0-14 hrs in a day. The maximum WT_1 power attains in 7 KW at 0-14 hrs in a day. WT_2 attains the maximum power of 6.8 KW at 0-14 hrs in a day. The battery charging time is 0-8 hrs, charged power range is 5 KW at 6hrs. The battery discharge time is 8-15 hr; it reached maximum discharged power is -5 KW at the time period of 10 hrs. The maximum grid power attains 2.5 KW at 20 hrs.

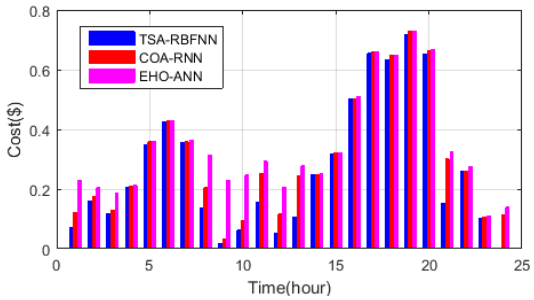

Figure 17: Cost Comparison of proposed and existing technique

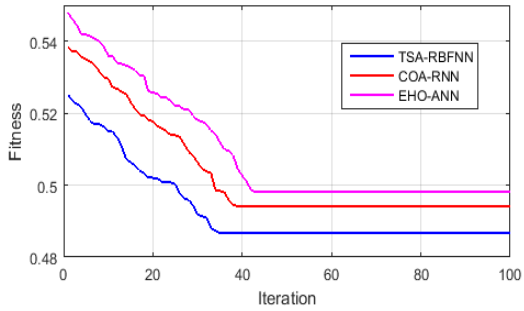

Figure 18: Fitness comparison of proposed and existing technique

Figure 17 illustrates that the cost comparison of different techniques. Sub plot 17 (a) indicates the cost comparison analysis of TSA-RBFNN with EHO-ANN; when comparing to this in our proposed TSA-RBFNN gives the better result.

Sub plot 17 (b) signifies the cost comparison analysis of TSA-RBFNN with CHO-RNN; when comparing to this in our proposed TSA-RBFNN gives the better result. In Figure 18, the fitness comparison of TSA-RBFNN with existing approaches is presented. Where, TSA-RBFNN approach in the range of iteration is 38 whereas the fitness value is 0.53. The existing COA-RNN technique in the range of iteration is 39 whereas the fitness value is 0.54, then the existing EHO-ANN technique in the range of iteration is 41 whereas the fitness value is 0.55. When likened with the existing approaches, the fitness of TSA-RBFNN approach is less.

Table 1: Statistical analysis of proposed and existing technique

Solution Techniques	Mean	Median	Standard Deviation (SD)
TSA-RBFNN	0.4933	0.4867	0.0111
COA-RNN	0.5032	0.4940	0.0142
BFA-ANN	0.5095	0.4981	0.0159

Table 2: Elapsed Time

Solution approaches	Elapsed Time(sec)
TSA-RBFNN	1.471046
COA-RNN	1.592524
BFA-ANN	1.871135

Table 1 tabulates the statistical analysis of TSA-RBFNN with existing method. The mean value of TSA-RBFNN technique is 0.4933, mean value of existing COA-RNN technique is 0.5032 and BFA-ANN is 0.5095. The median value of proposed TSA-RBFNN technique is 0.4867, mean value of existing COA-RNN technique is 0.4940 and BFA-ANN is 0.4981. The SD value of proposed TSA-RBFNN technique is 0.0111, mean value of existing COA-RNN technique is 0.0142 and BFA-ANN is 0.0159. Table 2 shows the elapsed time for TSA-RBFNN with existing technique. Here the elapsed time for TSA-RBFNN technique is 1.471046, the elapsed time for existing COA-RNN is 1.592524 and BFA-ANN is 1.871135.

6. CONCLUSION

This manuscript proposed a hybrid method for optimum energy management of a grid-connected PV, wind turbine, micro turbine including energy storage system using TSA-RBFNN technique. Here, the system model and the distribution of micro-grid with minimum effort using the TSA-RBFNN technique. The TSA-RBFNN technique chooses the allocation of micro-grid as represented by the load requirement along less fuel cost, replacement and operating cost. The advantages of the TSA-RBFNN approach were improved local search capability, minimized computation complex, randomness in generation, which provides maximized accuracy of dimension. TSA-RBFNN approach was examined for various load requirement values, micro-grid configuration and the corresponding annualized total costs were evaluated. The efficacy of the TSA-RBFNN technique was analyzed using the comparison of other existing approaches, such as COA-RNN and BFA-ANN. Finally, the comparison outcomes prove that the TSA-RBFNN technique was more proficient than the other existing techniques.

REFERENCES

[1] V. Bui, A. Hussain and H. Kim, **A Multiagent-Based Hierarchical Energy Management Strategy for Multi-Microgrids Considering Adjustable Power and Demand Response**, *IEEE Transactions on Smart Grid*, vol. 9, no. 2, pp. 1323-1333, Jun 2018.

[2] Z. Wang, B. Chen, J. Wang and J. kim, **Decentralized Energy Management System for Networked Microgrids in Grid-Connected and Islanded Modes**, *IEEE Transactions on Smart Grid*, vol. 7, no. 2, pp. 1097-1105, Jun 2016.

[3] G. Aghajani, H. Shayanfar and H. Shayeghi, **Presenting a multi-objective generation scheduling model for pricing demand response rate in micro-grid energy management**, *Energy Conversion and Management*, vol. 106, pp. 308-321, Dec2015.

[4] M. Hossain, H. Pota, S. Squartini and A. Abdou, **Modified PSO algorithm for real-time energy management in grid-connected microgrids**, *Renewable Energy*, vol. 136, pp. 746-757, Jun 2019.

[5] Y. Wang, Y. Huang, Y. Wang, H. Yu, R. Li and S. Song, **Energy Management for Smart Multi-Energy Complementary Micro-Grid in the Presence of Demand Response**, *Energies*, vol. 11, no. 4, p. 974, Apr 2018.

[6] S. Koko, K. Kusakana and H. Vermaak, **Optimal energy management of a grid-connected micro-hydrokinetic with pumped hydro storage system**, *Journal of Energy Storage*, vol. 14, pp. 8-15, Dec 2017.

[7] K. Kusakana, **Optimal operation scheduling of grid-connected PV with ground pumped hydro storage system for cost reduction in small farming activities**, *Journal of Energy Storage*, vol. 16, pp. 133-138, Apr 2018.

[8] H. Al Garni, A. Awasthi and M. Ramli, **Optimal design and analysis of grid-connected photovoltaic under different tracking systems using HOMER**, *Energy Conversion and Management*, vol. 155, pp. 42-57, Jan 2018.

[9] B. Olaszi and J. Ladanyi, **Comparison of different discharge strategies of grid-connected residential PV systems with energy storage in perspective of optimal battery energy storage system sizing**", *Renewable and Sustainable Energy Reviews*, vol. 75, pp. 710-718, Aug 2017.

[10] R. Dufo-López and J. Bernal-Agustín, **Techno-**

economic analysis of grid-connected battery storage, *Energy Conversion and Management*, vol. 91, pp. 394-404, Feb 2015.

[11] A. Keshtkar and S. Arzanpour, **An adaptive fuzzy logic system for residential energy management in smart grid environments**, *Applied Energy*, vol. 186, pp. 68-81, Jan 2017.

[12] M. Islam, F. Yang, C. Ekanayek and M. Amin, **Grid power fluctuation reduction by fuzzy control based energy management system in residential microgrids**, *International Transactions on Electrical Energy Systems*, vol. 29, no. 3, p. e2758, Mar 2018.

[13] N. Gupta and R. Garg, **Tuning of asymmetrical fuzzy logic control algorithm for SPV system connected to grid**, *International Journal of Hydrogen Energy*, vol. 42, no. 26, pp. 16375-16385, Jun 2017. Available: 10.1016/j.ijhydene.2017.05.103.

[14] M. Rouholamini and M. Mohammadian, **Heuristic-based power management of a grid-connected hybrid energy system combined with hydrogen storage**, *Renewable Energy*, vol. 96, pp. 354-365, Oct 2016.

[15] K. Kusakana, **Energy management of a grid-connected hydrokinetic system under Time of Use tariff**, *Renewable Energy*, vol. 101, pp. 1325-1333, Feb 2017.

[16] X. Han, H. Zhang, X. Yu and L. Wang, **Economic evaluation of grid-connected micro-grid system with photovoltaic and energy storage under different investment and financing models**, *Applied Energy*, vol. 184, pp. 103-118, Dec 2016.

[17] A. Ouai, L. Mokrani, M. Machmoum and A. Houari, **Control and energy management of a large scale grid-connected PV system for power quality improvemen**, *Solar Energy*, vol. 171, pp. 893-906, Sep 2018.

[18] Y. Li, W. Gao and Y. Ruan**, Performance investigation of grid-connected residential PV-battery system focusing on enhancing self-consumption and peak shaving in Kyushu, Japan**, *Renewable Energy*, vol. 127, pp. 514-523,Nov 2018.

[19] H. Pourvali Souraki, M. Radmehr and M. Rezanejad, **Distributed energy storage system-based control strategy for hybrid DC/AC microgrids in grid-connected mode**, *International Journal of Energy Research*, vol. 43, no. 12, pp. 6283-6295, Oct 2018.

[20] N. Chettibi and A. Mellit, **Intelligent control strategy for a grid connected PV/SOFC/BESS energy generation system**, *Energy*, vol. 147, pp. 239-262, Mar 2018.

[21] N. Liu, L. He, X. Yu and L. Ma, **Multiparty Energy Management for Grid-Connected Microgrids With Heat- and Electricity-Coupled Demand Response**, *IEEE Transactions on Industrial Informatics*, vol. 14, no. 5, pp. 1887-1897, Sep 2018.

[22] D. Lifshitz and G. Weiss, **Optimal energy management for grid-connected storage systems**, *Optimal Control Applications and Methods*, vol. 36, no. 4, pp. 447-462, Jul 2014.

[23] D. Arcos-Aviles, J. Pascual, L. Marroyo, P. Sanchis and F. Guinjoan, **Fuzzy Logic-Based Energy Management System Design for Residential Grid-Connected Microgrids**, *IEEE Transactions on Smart Grid*, vol. 9, no. 2, pp. 530-543, Apr 2018.

[24] U. Manandhar et al., **Energy Management and Control for Grid Connected Hybrid Energy Storage System Under Different Operating Modes**, *IEEE Transactions on Smart Grid*, vol. 10, no. 2, pp. 1626-1636, Nov 2019.

[25] H. Wu, S. Wang, B. Zhao and C. Zhu, **Energy management and control strategy of a grid-connected PV/battery system**, *International Transactions on Electrical Energy Systems*, vol. 25, no. 8, pp. 1590-1602, Aug 2014.

[26] P. Malysz, S. Sirouspour and A. Emadi, **An Optimal Energy Storage Control Strategy for Grid-connected Microgrids**, *IEEE Transactions on Smart Grid*, vol. 5, no. 4, pp. 1785-1796, Jun 2014.

[27] D. Arcos-Aviles, J. Pascual, F. Guinjoan, L. Marroyo, P. Sanchis and M. Marietta, **Low complexity energy management strategy for grid profile smoothing of a residential grid-connected microgrid using generation and demand forecasting**, *Applied Energy*, vol. 205, pp. 69-84, Nov 2017.

[28] S. Nojavan, M. Majidi and K. Zare, **Performance improvement of a battery/PV/fuel cell/grid hybrid energy system considering load uncertainty modeling using IGDT**, *Energy Conversion and Management*, vol. 147, pp. 29-39, Sep 2017.

[29] R. Lingamuthu and R. Mariappan, **Power flow control of grid connected hybrid renewable energy system using hybrid controller with pumped storage**, *International Journal of Hydrogen Energy*, vol. 44, no. 7, pp. 3790-3802, Feb 2019.

[30] Y. Hu and L. Chen, **A nonlinear hybrid wind speed forecasting model using LSTM network, hysteretic ELM and Differential Evolution algorithm**, *Energy Conversion and Management*, vol. 173, pp. 123-142, Oct 2018.

[31] K. Lin, P. Pai and Y. Ting, **Deep Belief Networks With Genetic Algorithms in Forecasting Wind Speed**, *IEEE Access*, vol. 7, pp. 99244-99253,Jul 2019.

[32] Y. Wang, Y. Shen, S. Mao, G. Cao and R. Nelms, **Adaptive Learning Hybrid Model for Solar Intensity Forecasting**, *IEEE Transactions on Industrial Informatics*, vol. 14, no. 4, pp. 1635-1645, Jan 2018.

[33] A. Ahmad, N. Javaid, M. Guizani, N. Alrajeh and Z. Khan, **An Accurate and Fast Converging Short-Term Load Forecasting Model for Industrial Applications in a Smart Grid**, *IEEE Transactions on*

Industrial Informatics, vol. 13, no. 5, pp. 2587-2596, Dec 2017.

[34] S. Pulipaka and R. Kumar, **Power prediction of soiled PV module with neural networks using hybrid data clustering and division technique**, *Solar Energy*, vol. 133, pp. 485-500, Aug 2016.

[35] S. Kaur, L. Awasthi, A. Sangal and G. Dhiman, **Tunicate Swarm Algorithm: A new bio-inspired based metaheuristic paradigm for global optimization**, *Engineering Applications of Artificial Intelligence*, vol. 90, p. 103541, Apr 2020.

[36] R. Liu, Y. He, Y. Zhao, X. Jiang and S. Ren, **Tunnel construction ventilation frequency-control based on radial basis function neural network**, *Automation in Construction*, vol. 118, p. 103293, Oct 2020.